

Design and Fabrication of a Multi-Axis MEMS Force Sensor with Integrated Carbon Nanotube Based Piezoresistors

Michael A. Cullinan, Robert M. Panas and Martin L. Culpepper

Massachusetts Institute of Technology, Department of Mechanical Engineering
77 Massachusetts Avenue, Room 35-135, Cambridge, Massachusetts, USA
Email: mcullin1@mit.edu, rpanas@mit.edu, culpepper@mit.edu

ABSTRACT

Carbon nanotube-based strain sensors have the potential to overcome many of the limitations in small-scale force/displacement sensing technologies due to their small size and high strain sensitivity. In this paper, we will present the design and fabrication of a multi-axis MEMS force sensor with integrated carbon nanotube based piezoresistive sensors. We will show that through proper sensor design and fabrication it is possible to improve the performance of these sensors by several orders of magnitude and produce nanoscale sensors with a dynamic range of greater than 80 dB. Overall, the force sensor presented in this paper has a resolution of 5.6 nN and a range up to 84 μ N.

Keywords: Carbon Nanotube, Force Sensor, Piezoresistor, MEMS, HexFlex

1 INTRODUCTION

Multi-axis force sensing is required in biology, materials science, and nanomanufacturing. Unfortunately, few fine-resolution, multi-axis MEMS force sensors exist because their creation involves substantial design and manufacturing challenges. In this paper, we will present the design and fabrication of a 3-axis MEMS force sensor used to measure the adhesion forces between an array of cells and a surface. This is important in the development of biomedical implants because it will allow researchers to determine the suitability of different types of materials both for areas where cell growth is desired and for areas where there should be no cell growth.

MEMS force sensors tend to rely on one of three sensing methods: capacitive sensing, optical laser detection, and piezoresistive sensing. Several multi-axis force sensors have been developed using capacitive sensors [1,2]. These sensors are difficult to fabricate and require relatively large sensor areas (mm^2) for each axis in order to achieve high force resolution. This makes capacitive sensing impractical for small, inexpensive, multi-axis force sensors. Optical sensors are widely used in atomic force microscopy (AFM) to make high resolution force measurements in one axis. Optical sensors are rarely used in microscale, multi-axis sensing due to the difficulty and cost of integrating multiple sets of optics into a small region. Also, optical sensors

require relatively large lasers which make it impossible to miniaturize the force sensing system to the micro-scale. Piezoresistive sensors offer the most promise at the micro-scale due to their small size and relative ease of integration into MEMS devices. Piezoresistive transducers are commonly found in MEMS devices such as pressure sensors, accelerometers, and AFM cantilevers [3]. Several dual-axis MEMS cantilevers with nN-level resolution have previously been demonstrated [4,5].

2 FORCE SENSOR DESIGN

Multi-axis, precision force sensing is needed to measure adhesion forces between cells and various material surfaces. For example, these measurements enable one to know (i) how well cells bond to different types of biomedical implant materials and (ii) the effects that drug coatings have on the prevention/promotion of adhesion. This type of measurement is necessary where the mechanical properties of the cell-implant interface are critical [6].

The multi-axis force sensor presented in this paper is designed to fit on top of a Hexflex nanopositioner as seen in Figure 1 [7].

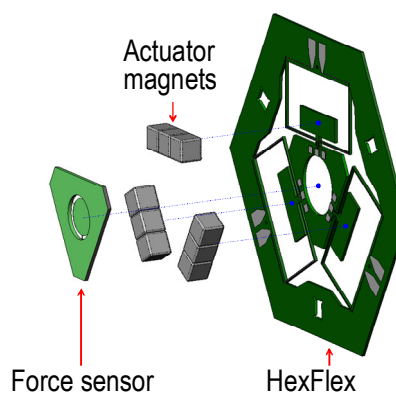


Figure 1. Exploded view of Hexflex-force sensor assembly.

In this setup, the HexFlex nanopositioner is used to precisely move the multi-axis force sensor. The precise, six degree-of-freedom motion of the HexFlex is necessary to properly position the force sensor into place and align the center stage of the force sensor with the surface of the cells. The HexFlex can then be used to lower the force sensor stage into contact with the cells and to make sure even

pressure is applied over the entire cell array. After the cells bond to the center stage of the force sensor, the HexFlex can be used to slowly retract the force sensor from the surface to which the cells are adhered. Using feedback from the force sensor, the HexFlex can be used to compensate for any torques that might be applied to the cells during this retraction phase and to ensure that only the direct force normal to the cell surface is being measured. Overall, this setup and procedure makes it possible to accurately and precisely quantify the adhesion forces between cells and different types of surfaces.

2.1 Functional Requirements

Accurate measurement of cell adhesion forces between surfaces requires multi-axis sensing to make sure that the surfaces are suitably positioned and oriented, thereby ensuring that load is applied evenly over the surfaces during testing. Cellular adhesion forces are typically on the scale of nN's [8]. When thousands of cells are arrayed on the surface being tested, the adhesion force is on the order of 100's of μ N. Therefore, to be useful, the force sensor must have 100's of μ N range and nN level resolution. The natural frequency of the force sensor was set to 1 kHz in order to ensure that it was capable of operating at least 1 order of magnitude faster than the HexFlex, which has a natural frequency of \sim 100 Hz. This ensures that the force sensor can be used in feedback mode with the HexFlex, even when the HexFlex is operating at its maximum speed. In addition, in order to ensure that the force sensor is applying an uniform force over the entire cell array, the force sensor must be capable of measuring forces perpendicular to the plane of contact (Z) and torques about axes that are parallel to the planes of contact, (θ_x , θ_y). Also, the force sensor must fit on the central stage of the Hexflex and the force sensor must be low cost (<\$100) so that it can be replaced after each test. These functional requirements are summarized in Table 1.

Functional Requirement	Value
Measurement Axis	Z, θ_x , θ_y
Range	100's of μ N
Resolution	\sim 1 nN
Natural Frequency	1 kHz
Cost	< \$100
Footprint	< 1 mm ²

Table 1: Force Sensor Functional Requirements.

2.2 CNT-Based Force Sensor Design

A comprehensive system level noise model was used to design the CNT-based force sensor. The force sensor is comprised of three coplanar flexures with integrated CNT-based piezoresistive sensors at the base of the flexures. The piezoresistors are in a quarter bridge arrangement. A full Wheatstone bridge was not used due to fabrication and

thermal heating constraints. The CNT-based piezoresistors are connected to aluminum contact pads on the outer base of the force sensor via aluminum traces. The sensors are placed at the base of the structure to maximize the strain imposed upon the resistors. A schematic of the CNT-based piezoresistive force sensor is given in Figure 2.

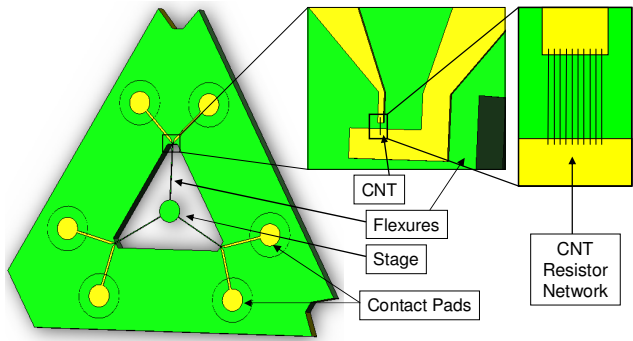


Figure 2. 3-axis force sensor with CNT-based piezoresistors.

The final flexure dimensions of the force sensor are a beam length of 2.5 mm, a beam width of 35 μ m and a beam thickness of 10 μ m. Based on this design it was estimated that the CNT-based piezoresistive force sensor should have a force resolution of approximately 100 μ N and a resolution of approximately 7 nN. This works out to a dynamic range of 83 dB. In addition, the estimated natural frequency was approximately 1000 Hz. These design properties are presented in Table 2.

Property	Value
Beam Length	2.5 mm
Beam Width	35 μ m
Beam Thickness	10 μ m
Maximum Force	100 μ N
Natural Frequency	1 kHz
Dynamic Range	83 dB

Table 2: CNT-Based Force Sensor Design.

3 FORCE SENSOR FABRICATION

The CNT-based MEMS force sensors were fabricated using a combination of conventional microfabrication and self assembly techniques. The process starts with a 150 mm silicon-on-insulator (SOI) wafer with a 10 μ m device layer, a 500 μ m handle layer, and a 1 μ m oxide layer. First, an RCA clean is used to remove any contaminants from the wafer surface. Next, the wafer is placed in the oxide furnace and 300 nm of thermal oxide is grown on the wafer.

After this high temperature processing step is completed, a protective photoresist coating is applied to the front side of the wafer and the back side polysilicon is removed. Next, 500 nm of aluminum is sputtered onto the wafer. Photolithography is used to define the wire traces

and bond pads while etching is used to remove the excess aluminum from the wafer.

Next, a protective photoresist is applied to the front side of the wafer so that it is not damaged while a buffered oxide etch (BOE) is used to remove the thermal oxide from the back side of the wafer. After this step, photolithography with is used to define the flexure structure on the front side of the wafer. A BOE is used to remove the oxide from the front side of the wafer and deep reactive ion etching (DRIE) is used to create the flexures in the device layer of the SOI wafer.

Finally, photolithography is used to pattern the back side of the wafer. The front side of the wafer is then mounted to a quartz handle wafer. This handle wafer acts as both a protective layer for the front side as well as a mechanical structure that holds the wafer together after the DRIE step. DRIE is used to etch the back side of the wafer and to release the flexures from the handle layer of the SOI wafer. DRIE is also used to etch through the entire wafer in order to separate the wafer into devices. After the DRIE step, a vapor hydrofluoric acid (HF) step is used to remove the excess oxide from the insulating layer of the SOI wafer and the wafer is placed into an acetone bath to separate the chips from the quartz wafer.

After the microfabrication is complete, CNT-based piezoresistors are deposited onto the blank CNT force sensors using dielectrophoresis. A droplet of a 3 g/L CNT solution is placed on the gap between the electrodes on the force sensor structure. A 5V peak-to-peak ac voltage with a frequency of 5 MHz is used to align the CNTs between the two electrodes. This deposition process is continued for 15 minutes in order to ensure that the maximum number of CNTs are deposited on the force sensor structure. After the sensors are deposited by dielectrophoresis, they are coated in an aluminum oxide protective layer and annealed at 525 °C for 30 minutes in order to minimize the amount of noise in the sensor. The final result of this fabrication process is shown in Figure 3.

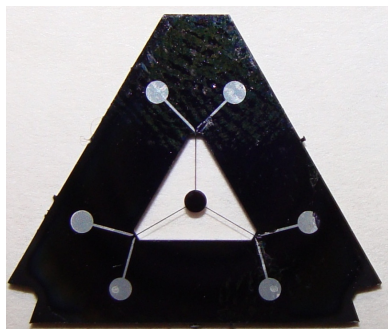


Figure 3. Fabricated 3-axis force sensor with CNT-based piezoresistors.

4 CALIBRATION

The force sensor is calibrated using a micrometer to actuate the center stage of the force sensor as shown in

Figure 4. The micrometer has a digital readout with a resolution of 1 μm . Spring pins are used to connect the bond pads on the force sensor to wires that run to the Wheatstone bridge circuit. These spring pins provide a preload to the force sensor to hold it in place during testing and ensure that all of the bond pads are in contact during testing. A small 1 mm diameter ball is connected to the tip of the micrometer head in order to ensure a small contact area and to prevent torques from being transmitted to the center stage from the rotation of the micrometer head.

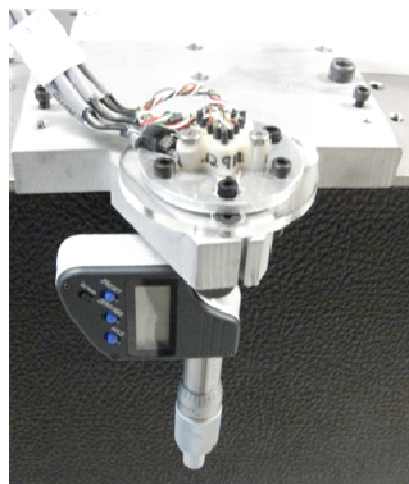


Figure 4. Force sensor calibration setup.

In order to calibrate the force sensor, the readout from each of the sensors was amplified through the Wheatstone bridge circuit and read into Labview. An initial measurement for all three sensors was taken, then the micrometer was actuated by 1 micron and a new set of measurements was recorded. This process was continued for 35 μm or until the force sensor reached about 1/3 of its predicted maximum displacement. The output of each sensor was recorded for each 1 micron displacement. These measurements were then used to create calibration curves for each piezoresistor in the force sensor.

5 RESULTS

The calibration results for each sensor are presented in Figure 5. Sensor 1 has a sensitivity of 0.79 mV per μN , while sensors 2 and 3 have sensitivities of 0.64 mV per μN and 0.59 mV per μN respectively. Each of these calibration curves explains over 95 percent of the variance in voltage with the increase in force applied to the structure. The differences in force sensitivities could be due to either the differences in the gauge factors of the sensors or to asymmetric loading of the structure by the micrometer. Previous results with the test structures have shown that the gauge factor of CNT-based piezoresistive sensors can vary by up to 12 percent. This explains about half of the variation between the sensors. Asymmetric loading of the force sensor by the micrometer could also contribute to the

difference in measured sensitivities by imposing torques onto the force sensor as well as z-axis displacement. These torques would cause some of the flexure beams to be strained more than others, which would result in the higher readouts from these sensors.

For example, a positive torque around the x-axis would result in an increased strain on sensor 1 but a decreased strain on sensors 2 and 3. Such a torque could be created if the location of the actuation was moved in the positive y-direction from the center of stiffness of the force sensor. Such an offset could either be created by small fabrication errors that result in the center of stiffness not being at the same location as the geometric center or by the actuator not pushing directly on the geometric center of the force sensor. Either way, this type of torque about the x-axis could help explain the remaining discrepancy between the measured sensitivities of each of the sensors.

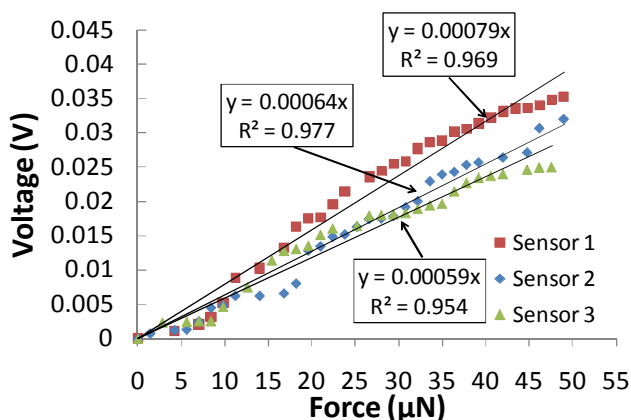


Figure 5. Calibration curve for each CNT-based sensor on the force sensor.

In addition to the linear calibration curves, each sensor appears to have a sinusoidal component. This component is likely due to thermal variations over the testing period. The total test took about 20 minutes, which is approximately equal to the thermal period of the room. Therefore, we would expect to see about 1 full thermal period in each sensor due to thermal variations of the room.

The total range of the system was measured by increasing the displacement of the micrometer head until a sharp change in the sensor readout was observed. This sharp change was caused by the fracture of one of the flexure beams, which caused the readout from the sensor on that flexure beam to return to its original value, since the strain on the CNT-based piezoresistors decreased to zero. Overall, the range of the sensor was measured to be about 60 microns. The stiffness of the force sensor measured from the nanoindentation tests was 1.4 N/m. Therefore the force range of the force sensor was measured to be 84 μ N.

The resolution of each sensor was calculated by dividing the noise in each sensor by the sensitivity of each sensor. The measured resolution for sensor 1 was 9.5 nN and it was 11.8 nN and 6.7 nN for sensors 2 and 3,

respectively. The results for each sensor along with the corresponding measured dynamic ranges for each sensor are presented in Table 6.5.

	Sensor 1	Sensor 2	Sensor 3
Sensitivity	790 V/N	640 V/N	590 V/N
Noise	7.5 μ V	7.5 μ V	4.0 μ V
Dynamic Range	78.4 dB	76.5 dB	81.3 dB

Table 6.5: Results for each piezoresistor in the force sensor.

The overall resolution of the force sensor is calculated by taking the weighted sum of squares of each of the three sensors in the force sensor structure. Based on this calculation, the resolution of the force sensor is approximately 5.6 nN. This corresponds to a dynamic range of 83 dB and matches the predicted dynamic range for the sensor of 83.2 dB with less than 0.25% error.

6 CONCLUSIONS AND FUTURE WORK

From these results, it is clear that the dynamic range of multi-axis MEMS sensors can be significantly improved through the use of carbon nanotube based piezoresistors. However, more work still needs to be done in order to maximize the dynamic range of these sensors. For example, the dynamic range of the force sensor can be improved by redesigning the force sensor system to increase the sensor area. Also, the force sensor could be improved by incorporating higher gauge factor CNTs into the sensor. Overall, these changes could help to increase the dynamic range of the force sensor to over 110 dB. Therefore, the force sensor could achieve a resolution of about 100 pN while maintaining the same range as the current CNT-based force sensor.

REFERENCES

- [1] F. Beyeler, S. Muntwyler, and B.J. Nelson, *Journal of Microelectromechanical Systems*, 18, 433-441 2009.
- [2] Y. Sun and B.J. Nelson, *Biomedical Materials*, 2, S16-S22, 2007.
- [3] M. Tortonese, R.C. Barrett, and C.F. Quate, *Applied Physics Letters*, 62, 834-836, 1993.
- [4] B. Chui, T. Kenny, H. Mamin, B. Terris, and D. Rugar, *Applied Physic Letters*, 72, 1388-1390, 1998.
- [5] T.C. Duc, J. Creemer, and P.M. Sarro, *IEEE Sensors Journal*, 7, 96-104, 2007.
- [6] W. Xue, B.V. Krishna, A. Bandyopadhyay, and S. Bose, *Acta Biomaterialia*, 3, 1007-1018, 2007.
- [7] C.M. Dibiasio and M.L. Culpepper, *Proceedings of the 2009 Annual Meeting of the American Society for Precision Engineering*, Monterey, CA: 2009.
- [8] K.J.V. Vliet, G. Bao, and S. Suresh, *Acta Materialia*, 51, 5881-5905, 2003.